| REPORT DOCUMENTATION PAGE | | Form Approved OMB No. 0704-0188 |
|---|---|---|

| 1. AGENCY USE ONLY (Leave blank) | 2. REPORT DATE 1995 | 3. REPORT TYPE AND DATES COVERED Interim |
|---|---|---|

| 4. TITLE AND SUBTITLE Solvent Effects on the Electronic Spectrum of Reichardt's Dye | 5. FUNDING NUMBERS N00014-90-J-1608 G |
|---|---|

**6. AUTHOR(S)**

Ricardo Bicca de Alencastro, Joaquim D. da Motta Neto and Michael C. Zerner

| 7. PERFORMING ORGANIZATION NAME(S) AND ADDRESS(ES) University of Florida Department of Chemistry Gainesville, FL 32611 USA | 8. PERFORMING ORGANIZATION REPORT NUMBER |
|---|---|

| 9. SPONSORING/MONITORING AGENCY NAME(S) AND ADDRESS(ES) Office of Naval Research Chemistry Division Code 1113 Arlington, VA 22217-5000 | 10. SPONSORING/MONITORING AGENCY REPORT NUMBER Technical Report 25 |
|---|---|

**11. SUPPLEMENTARY NOTES**

Published Intern. J. Quantum Chem.

| 12a. DISTRIBUTION/AVAILABILITY STATEMENT This document has been approved for public release: its distribution is unlimited. | 12b. DISTRIBUTION CODE |
|---|---|

**13. ABSTRACT** (Maximum 200 words)

See attached Abstract.

DTIC SELECTED APR 27 1995 B

19950427 013

DTIC QUALITY INSPECTED 3

| 14. SUBJECT TERMS | | | 15. NUMBER OF PAGES 28 |
|---|---|---|---|
| | | | 16. PRICE CODE |

| 17. SECURITY CLASSIFICATION OF REPORT Unclassified | 18. SECURITY CLASSIFICATION OF THIS PAGE Unclassified | 19. SECURITY CLASSIFICATION OF ABSTRACT Unclassified | 20. LIMITATION OF ABSTRACT SAR |
|---|---|---|---|

OFFICE OF NAVAL RESEARCH

GRANT or CONTRACT N00014-90-J-1608

R&T CODE 4131057- - - 01

Technical Report No. 25

Solvent Effects on the Electronic Spectrum of Reichardt's Dye

by

Ricardo Bicca de Alencastro, Joaquim D. da Motta Neto and Michael C. Zerner

Prepared for Publication or Published

in the

Intern. J. Quantum Chem.

University of Florida
Department of Chemistry
Quantum Theory Project
Gainesville, FL 32611-8435

April 18, 1995

# Solvent Effects on the Electronic Spectrum of Reichardt's Dye

Ricardo Bicca de Alencastro

*Physical Organic Chemistry Group, lab. A622, Departamento de Química Orgânica, Instituto de Química da UFRJ, Cidade Universitária, CT, Bloco A, Rio de Janeiro, RJ 21949–900, Brasil*

Joaquim D. da Motta Neto and Michael C. Zerner

*Quantum Theory Project, PO Box 1184–35, Williamson Hall, University of Florida, Gainesville, Florida 32611, USA*

# ABSTRACT

The extreme sensitivity of the absorption spectrum to small changes in the medium polarity has made Reichardt's dyes useful molecular probes in the study of micelle/solution interfaces and phospholipid bilayers. This work reports preliminary results of semiempirical quantum chemical calculations on some conformations of 2,6-diphenyl-(2,4,6-triphenyl-1-pyridinium)-*N*-phenoxide betaine (Reichardt's betaine, RB), which exhibits negative solvatochromic effects. We have used the AM1 Hamiltonian of Dewar in the geometry optimizations, and the Intermediate Neglect of Differential Overlap method parameterized for spectroscopy (INDO/S). For RB, two low-lying conformations have been found. The small difference in energy between them suggests that both forms may be present in solution, an observation confirmed by calculations on the spectra using the SCRF model: the superposition of the calculated spectra for these two forms matches the experimental spectra very well. For non-polar solvents, the general pattern consists of variation of Et(30) concurrent with variation of the dielectric constant. We have also carried out calculations for solvents which form specific (e.g. H-bond) binding to the solute, namely methanol and water, using a supermolecule approach. Our results are in excellent agreement with the experiment and present an accurate description of the spectra.

# KEY WORDS

# 1. Introduction

The absorption and emission spectra of a substance change characteristics (positions and intensities) on going from the gas phase to solution. These differences largely depend on the solvent and, although they are generally small, they can be very large in some cases [1–3]. This phenomenum is widely known as *solvatochromism* and was first recognized more than one hundred years ago by Kundt [1]. It occurs because dissolved molecules interact differently with the environment in their ground and several excited states. These interactions are not always easily described and this subject has been intensely pursued in the last 40 years: dozens of books and accounts, and innumerable reports have been devoted to it. For empirical approaches, the interested reader will find useful material in references [3–5], and for a thorough description of theoretical and computational aspects, in references [6–7], among many others. From the empirical point of view, solvatochromism has been used to construct linear solvation free energy relationships (LSER) that give access to solvent properties important to explain several important physicochemical phenomena as, for example, chemical kinetics, conformation or tautomeric equilibria, and even partition coefficients [3,4].

The problem of theoretically predicting the electronic properties of organic substances and their observed spectra in solution has interested and challenged theoretical chemists for more than four decades. This field has been very active especially in the last few years and Rauhut, Clark and Steinke [8] have recently given a summary of recent literature. Following recent work in this lab on solvent effects [9] we decided to examine the electronic spectrum of one of the most widely used solvatochromic dyes, 2,6–diphenyl-(2,4,6–triphenyl-1–pyridinium)-*N*-phenoxide (Reichardt's betaine #1, a.k.a. Reichardt's dye #1, RB, Figure 1) [10–18]. The lowest energy band of RB undergoes a negative solvatochromism (hipsochromic shift) of about 360 nm (approximately 10,000 cm$^{-1}$) in going from diethyl ether to water. This is the basis of the very popular $E_T(30)$ scale (or its equivalent $E_T^N$ scale) [3–5, 10–16].

1

## 2. Method

We initially performed a search of low lying conformations of RB with geometry optimizations at the SCF level using the AM1 [19–21] model Hamiltonian, within the AMPAC package [22]. Keywords PRECISE and GNORM=0.05 were used in order to obtain the smallest residual gradient possible. Solvent effects were included in our study at two levels: in a first approximation, the bulk was simulated by a self-consistent reaction field (SCRF) within the continuum model [23–28]. We use in this work the SCRF formulation as given by Karelson and Zerner [9]: in model A of this reference, we write the energy of the universe (molecule + environment) as

$$E_u = E^0 - \frac{1}{2} \cdot (1 - \frac{1}{\epsilon}) \frac{Q^2}{a_0} - \frac{1}{2} \cdot \vec{\vec{g}}(\epsilon, a_0) < \psi|\vec{\mu}|\psi > < \psi|\vec{\mu}|\psi > \qquad (1)$$

with $Q$ the net charge of the solute and $\vec{\vec{g}}$ the reaction field tensor. We now form the functional

$$L = E^0 - \frac{1}{2} \cdot (1 - \frac{1}{\epsilon}) \frac{Q^2}{a_0} - \frac{1}{2} \cdot \vec{\vec{g}}(\epsilon, a_0) < \psi|\vec{\mu}|\psi > < \psi|\vec{\mu}|\psi > - W \cdot (< \psi|\psi > -1) \quad (2)$$

with $W$ the Lagrange multiplier ensuring normalization and $E_0$ the gas phase energy

$$E^0 = < \psi|H_0|\psi > \qquad (3)$$

where $H_0$ is the Hamiltonian for the isolated solute molecule. Applying the variational theorem to equation (2) leads to the Schrödinger equation for the state $|\psi >$

$$(H_0 - \vec{\vec{g}} < \psi|\vec{\mu}|\psi > < \vec{\mu} >)|\psi > = W \cdot |\psi > \qquad (4)$$

with the Fock operator for the electron k given by

$$f(k) = f_0(k) - \vec{\vec{g}} \cdot < \psi|\vec{\mu}|\psi > \cdot \mu(k) \qquad (5)$$

and the energy of the universe is then

$$E_u = W + E_{c,c} = W + \frac{1}{2} \vec{\vec{g}} \cdot |< \psi|\vec{\mu}|\psi > |^2 \qquad (6)$$

2

where the "solvent cost" $E_{c,c}$ is a correction that express the energy lost by the solvent in dissolving the solute. Note that the nuclear repulsion energy and the Born term,

$$\sum_A \sum_{B>A} \frac{Z_A Z_B}{R_{AB}} - \frac{1}{2} \cdot (1 - \frac{1}{\epsilon}) \frac{Q^2}{a_0} \; , \tag{7}$$

must be added. In this work we use an alternative procedure that includes the solvent relaxation, model B of reference [9]: we put a *second* Lagrange constraint in equation (2) such that

$$(H_0 - \frac{1}{2} \cdot \vec{g} \cdot <\psi|\vec{\mu}|\psi><\vec{\mu}>)|\psi> = W \cdot |\psi> \tag{8}$$

and the Fock operator for electron k turns out to be

$$f(k) = f_0(k) - \frac{1}{2} \cdot \vec{g} \cdot <\psi|\vec{\mu}|\psi> \vec{\mu}(k) \tag{9}$$

an operator that yields equation (1) directly (since the interaction term includes the 1/2 ). The cavity radius $a_0$ (6.02 A for isolated RB) was determined from mass density. In addition, when necessary, we have also used the supermolecule approach [29–31] by including at least two solvent molecules around the solute (RB).

The absorption spectra were obtained (at the AM1 and AM1–SCRF geometries) by the spectroscopic version of the Intermediate Neglect of Differential Overlap (INDO/S) method [32–37]. The two center, two electron integrals are obtained from the modified Mataga-Nishimoto formula [38]

$$\gamma_{AB} = \frac{f_\gamma}{2f_\gamma/(\gamma_{AA} + \gamma_{BB}) + R_{AB}} \tag{10}$$

in which the Weiss parameter $f_\gamma$ was chosen equal to 1.2 in order to reproduce the spectrum of aromatic compounds [32]. The configuration interaction (CI) calculations included all single excitations from the 19 highest occupied MO's to the 12 lowest unoccupied MO's, plus the ground state, a total of 229 configurations.

# 3. Results and Discussion

*Results in gas phase (AM1)*

Table I presents a summary of our AM1 results for RB. Conformers A (Figure 2) and A'

differ only by a rotation of one of the phenyl rings by about 180 degrees, and have virtually

the same energy. Conformer B (Figure 3) was calculated to be 0.1 kcal/mol more stable in gas

phase, and this suggests that these conformers coexist in gas phase. In solution (under the SCRF

approximation [23–28]), differences between A, A' and B conformers are less than 1 kcal/mole on

going from ethanol to water. This suggests that these conformers likely also coexist in solution.

If this is the case, then the observed spectral properties must arise from a combination of the

spectral properties of all conformers. We assumed that the contributions of both forms should

be approximately the same (regardless of the existence of other conformations), so the observed

spectra are compared in this paper with the average of the spectra of the two forms, A and B.

The INDO/S-CIS calculated spectrum of RB in gas phase is shown in Tables II (Conformer

A, Figure 2) and III (Conformer B, Figure 3). There is no gas phase spectrum available in the

literature (there is little vapor pressure), so we compare our gas phase calculations to the results

obtained for a non polar solvent, namely, 1,4–dioxane [3], and recognize the limitations of this

comparison. In gas phase, the lowest excited singlet state is mostly HOMO→LUMO and was

calculated at 11,480 cm$^{-1}$ (Conformer A) and 11,220 cm$^{-1}$ (Conformer B), to be compared to

the experimental value of 12,580 cm$^{-1}$ in 1,4–dioxane [3, 10–18].

A broad shoulder is observed between about 20,000–22,200 cm$^{-1}$. We assign it to our next

two calculated transitions: HOMO→LUMO+1, calculated at 17,140 cm$^{-1}$ (conformer A) and

16,920 cm$^{-1}$ (conformer B), and HOMO-1→LUMO, calculated at 24,180 cm$^{-1}$ (conformer

A) and 24,690 cm$^{-1}$ (conformer B). Both of these excitations are of medium strength. Their

oscillator strength average is at about 19,400 cm$^{-1}$, to be compared to the observed maximum

4

of the shoulder at about 21,000 cm$^{-1}$ in 1,4–dioxane [3, 10–18]. The next observed peak is at 25,000 cm$^{-1}$ and is strong. This compares very well with calculated values of 25,560 cm$^{-1}$ (conformer A) and 25,190 cm$^{-1}$ (conformer B).

Finally, we consider a broad, intense band, observed with maximum at 32,260 cm$^{-1}$ with a slight shoulder at 30,300 cm$^{-1}$. Both conformers are calculated to have a great many transitions in this region. At about 31,500 cm$^{-1}$ (317 nm), both have strong transitions and both have strong transitions at about 34,500 cm$^{-1}$. Experimentally this band shows little solvent shift [3].

We conclude that the absorption spectrum as a whole is well described, as one can seen by comparing Tables II and III with the observed spectrum of RB in 1,4–dioxane [3]. The most important peak for our purposes is the first, observed at 10,500 cm$^{-1}$ [3]. We calculate 11,480 cm$^{-1}$ for conformer A and 11,220 cm$^{-1}$ for conformer B.

*Solvent effects: 1,4–dioxane*

Our next step was the consideration of solvent effects. One of our immediate goals was to establish the procedure that could be applied to a large number of solvents, in order to reproduce Reichardt's $E_T(30)$ scale [3–5, 10–16] and to check our understanding of this scale. For the non-polar solvents, that have no specific bonding with the solute (RB), the continuum approximation [23–28] should be enough to reach agreement with the observed spectra. However, we have to apply some caution, because even for the non-polar solvents the dielectric constant variation does *not* concur with the polarity of the solvent that is expressed by the $E_T(30)$ parameter. For example, 1,4–dioxane ($\epsilon=2.209$) is more polar than benzene ($\epsilon=2.284$) and acetonitrile ($\epsilon=35.94$) is more polar than DMSO ($\epsilon=46.45$) on the $E_T(30)$ scale.

The INDO/S-CIS calculated spectra of RB (conformations A and B) in 1,4–dioxane treated by the SCRF approach [9] are shown in Tables IV and V. The first band is calculated at 10,591 cm$^{-1}$ (for A) and 11,871 cm$^{-1}$ (for B). If we take the result for B (based on the fact that

5

the intensity is twice as large), the agreement with the experiment (12,600 cm$^{-1}$ [3, 10–16]) is very good.

A second band was calculated at 567 nm = 17,640 cm$^{-1}$ (conformer A) and 550 nm = 18,193 cm$^{-1}$ (conformer B), and accounts for a shift of about 600–900 cm$^{-1}$ from the gas phase result (see above). Again, the relation between oscillator strengths enables us to assign this band to the shoulder with maximum at about 21,000 cm$^{-1}$.

Comparison of Tables II — V show that the third and fourth transitions undergo an inversion from gas phase to solution. A third transition (HOMO→LUMO+4, HOMO→LUMO+8) is now calculated at 25,220 cm$^{-1}$ (conformer A) and 24,925 cm$^{-1}$ (conformer B). Both numbers match very well the sharp peak observed at approximately 25,000 cm$^{-1}$ = 400 nm.

Again we found a series of five very weak transitions beginning at 370 nm (including a n→π$^{*}$ transition from the lone pair of oxygen). This system is not observed in 1,4–dioxane, but the band appears in acetonitrile, and helps demonstrate the consistency of our assignments. Finally, the large, broad band calculated to begin at 330 nm is nearly unshifted with respect to the gas phase spectrum (compare Table II with IV, and Table III with V).

*Other non polar solvents: the special case of chloroform*

Other solvents in this range of $E_T(30)$ follow the same pattern: in general, increase of the dielectric constant is followed by an increase in the transition energy of the first band. Therefore, we simply give the calculated values in Table VI, in order to avoid repetition. It is observed that the value of $E_T(30)$ for benzene is underestimated by ca. 2.0 kcal/mol (700 cm$^{-1}$). The solvents 1,4–dioxane and chloroform present us with a larger error (4.0–5.0 kcal/mole) in $E_T(30)$. Since this error is not systematic with that of benzene, we might speculate that very weak specific interactions begin to affect the pattern of the non-polar solvents. In order to check this hypothesis, we carried out an additional SM calculation on RB (conformer B) surrounded by four chloroform

molecules (we have chosen chloroform because the specific interactions — H-bond involving the CHCl$_3$ proton — were easier to figure out than for the case of 1,4-dioxane). The resulting spectrum is depicted in Table VII. Clearly the H-bond affects the n→$\pi^*$ CT transition, and the corrected value of $E_T(30)$ = 38.8 kcal/mol (see Table VII) closely matches the experiment. The sharp peak observed at 25,000 cm$^{-1}$ for 1,4-dioxane is now blue shifted by 1,000 cm$^{-1}$. Thus, we conclude that results from the SCRF are indeed perturbed for CHCl$_3$ (and probably also for 1,4-dioxane) due to specific binding, even though the H-bonding is quite weak.

*H-bonding solvents: methanol*

Inspecting the case of methanol is interesting because its dielectric constant ($\epsilon$=32.63) is very close to that of acetonitrile ($\epsilon$=35.94). Thus, at the SCRF approximation [23-28], the INDO/S-CIS calculations should yield almost the same spectra. This is, indeed, the case as one can see from inspection of Table VI. The calculated (SCRF only) transition energy of acetonitrile (12,830 cm$^{-1}$) is slightly larger than that of methanol (12,250 cm$^{-1}$), while experimentally the first n→$\pi^*$ band is observed at 19,420 cm$^{-1}$ = 515 nm (the solution is red) for methanol and 16,080 cm$^{-1}$ = 622 nm (green-blue) for acetonitrile [3]. These calculations illustrate the well known phenomenum of the saturation in the SCRF model as $\vec{g}(\epsilon)$ approach 1/2 as $\epsilon$ increases. Clearly the continuum model [23-28] alone is not satisfactory. To correct this we decided to include two methanol molecules near the oxide terminæ of RB, and two molecules near the positively charged nitrogen. This simple arrangement "fixes" the calculated spectrum for methanol, as shown in Tables VIII and IX. At the SCRF-SM level of approximation, the n→$\pi^*$, CT band is located at 15,070 cm$^{-1}$ for conformer A and 14,140 cm$^{-1}$ for conformer B. We further observe that the oscillator strength for this transition is drastically reduced (compared to the gas phase calculation). Also, the now stronger HOMO-1→LUMO transition was calculated at 19,220 cm$^{-1}$ for conformer A and 19,320 cm$^{-1}$ for conformer B. This accounts for a blue shift of 7,000 cm$^{-1}$ with respect to the SCRF result. The agreement with the experimental

value of 19,420 cm$^{-1}$ is very good.

*Water*

The absorption spectrum of RB in water should be the most difficult to reproduce, due to the special properties of the solvent. The INDO/S-CIS calculated spectra of RB surrounded by four water molecules are shown in Tables X (conformer A) and XI (conformer B). The n→π$^*$, CT band was calculated at 14,060 cm$^{-1}$ for conformer A and 13,980 cm$^{-1}$ for conformer B. As previously observed for methanol, this band loses its oscillator strength by at least one order of magnitude (compared to the gas phase result). The experimental spectrum shows a peak at 453 nm, and this peak should be the one related to the $E_t(30)$ scale. However, based on the results of this paper, we now conclude that the observed peak (for methanol and water, and probably also for ethanol) rather corresponds to the second n→π$^*$ transitions, HOMO-1→LUMO for methanol (see Tables VIII and IX) and HOMO→LUMO+1 for water (see Tables X and XI). We also observe that for both solvents the sharp peak (observed close to 25,000 cm$^{-1}$ for 1,4–dioxane) is red shifted by about 1,000 cm$^{-1}$.

## 4. Concluding Remarks

In this work we have examined the absorption spectra of a compound which presents negative solvatochromism, Reichardt's dye #1 (RB). The challenge was to obtain a correct description of the negative solvatochromism exhibited by RB. For non-polar solvents, which make no specific binding to the solute, the continuum model [23–28] was enough to reproduce the experimental spectra. For solvents which form specific binding (e.g. H-bond) with RB, we had to apply the supermolecule approach [29–31]. This work provided basis from drawing some conclusions, that we now present.

(i) AM1 calculations have provided two low lying conformers very close in heats of formation, which suggests that they coexist, both in gas phase and in solution. (ii) We have

confirmed that the first CT band in the spectrum of RB has $n\rightarrow\pi^*$ character and arises from an excitation from the lone pair of the phenoxide oxygen. (iii) For non-polar solvents increase of the dielectric constant gives rise to increase of $E_t(30)$. (iv) For some non-polar solvents such as chloroform and 1,4–dioxane, specific binding, although quite weak, is enough to disturb the mentioned pattern and the CT band is further blue shifted. (v) One of the effects of the SCRF on the CI calculations is that the lowest energy $n\rightarrow\pi^*$, CT band loses its intensity as the dielectric constant increases. (vi) We observe that this effect holds even for SM calculations, so the bands used in the $E_t(30)$ scale for methanol and water are actually due to the second $n\rightarrow\pi^*$ transition. Finally, (vii) the INDO/S-CIS technique proved a successful tool in reproducing the empirical $E_t(30)$ scale. We summarize these results in Table VI and Figure 7. Perhaps slight discrepancies could be removed by increasing the number of solvent molecules, but we are more likely at the limit of the model we use for structure and spectroscopy.

## 5. Acknowledgements

# References

1. W. Liptay, *Angew. Chem.* **8**(3), 177–188 (1969).

2. N. Mataga and T. Kubota, *Molecular Interactions and Electronic Spectra*, M. Dekker Inc., New York, 1970.

3. C. Reichardt, *Solvents and Solvent Effects in Organic Chemistry*, 2nd ed., VCH Publishers, Weinheim, 1988.

4. O. Pytela, *Coll. Czech. Chem. Commun.* **53**, 1333–1400 (1988).

5. E.M. Kosower, *An Introduction to Physical Organic Chemistry*, Wiley, New York, 1968.

6. I.G. Kaplan, *Theory of Molecular Interactions: Studies in Phys. Theor. Chem.* **42**, Elsevier Publishers, Amsterdam, 1986.

7. M.P. Allen and D.J. Tildesley, *Computer Simulation of Liquids*, Oxford Univ. Press, Oxford (1989).

8. G. Rauhut, T. Clark and T. Steinke, *J. Am. Chem. Soc.* **115**(20), 9174–9181 (1993).

9. M.M. Karelson and M.C. Zerner, *J. Phys. Chem.* **96**(17), 6949–6957 (1992).

10. K. Dimroth, C. Reichardt, T. Siepmann and F. Bohlmann, *Liebigs Ann. Chem.* **661**, 1 (1963).

11. K. Dimroth and C. Reichardt, *Liebigs Ann. Chem.* **727**, 93 (1969).

12. C. Reichardt, *Liebigs Ann. Chem.* **752**, 64 (1971).

13. C. Reichardt and E. Harbusch-Görnert, *Liebigs Ann. Chem.* **1983**, 721 (1983)

14. C. Laurence, P. Nicolet, M. Lucon and C. Reichardt, *Bull. Soc. Chim. Fr.* **1987**(1), 125–130.

15. C. Laurence, P. Nicolet, M. Lucon and C. Reichardt, *Bull. Soc. Chim. Fr.* **1987**, 1001.

16. C. Reichardt, G. Schäfer and P. Milart, *Collect. Czech. Chem. Commun.* **55**, 97–107 (1990).

17. W. Linert and R.F. Jameson, *J. Chem. Soc. Perkin Trans.* **2**(8), 1415–1421 (1993).

18. W. Linert, B. Strauss, E. Herlinger and C. Reichardt, *J. Phys. Org. Chem.* **5**, 275–284 (1992).

19. M.J.S. Dewar, E.G. Zoebisch, E.F. Healy and J.J.P. Stewart, *J. Am. Chem. Soc.* **107**(13), 3902–3909 (1985).

20. M.J.S. Dewar and E.G. Zoebisch, *J. Mol. Struct. (Theochem)* **180**, 1 (1988).

21. A.A. Voityuk, *J. Struct. Chem.* **29**(1), 120 (1988).

22. AMPAC 2.1, authors D.A. Liotard, E.F. Healy, J.M. Ruiz and M.J.S. Dewar, Austin (1989).

23. O. Tapia and O. Goscinski, *Mol. Phys.* **29**(6), 1653–1661 (1975).

24. S. Miertuš, E. Scrocco and J. Tomasi, *Chem. Phys.* **55**, 117 (1981).

25. M.M. Karelson, T. Tamm, A.R. Katritzky, S.J. Cato and M.C. Zerner, *Int. J. Quantum Chem.* **37**, 1–13 (1990).

26. M.M. Karelson, T. Tamm, A.R. Katritzky, M. Szafran and M.C. Zerner, *Tetrahedron Comp. Meth.* **2**(5), 295–304 (1989).

27. D. Rinaldi, J.-L. Rivail and N. Rguini, *J. Comp. Chem.* **13**(6), 675–680 (1992).

28. O. Tapia, *J. Math. Chem.* **10**, 139–181 (1992).

29. D.L. Beveridge and G.W. Schnuelle, *J. Phys. Chem.* **78**(20), 2064–2069 (1974).

30. P. Claverie, J.P. Daudey, J. Langlet, B. Pullman, D. Piazzola and M.J. Huron, *J. Phys. Chem.* **82**(4), 405–418 (1978).

31. L.C.G. Freitas, R.L. Longo and A.M. Simas, *J. Chem. Soc. Faraday Trans* **88**(2), 189–193 (1992).

32. J. Ridley and M.C. Zerner, *Theor. Chim. Acta* **32**, 111–134 (1973).

33. M.C. Zerner, G.H. Loew, R.F. Kirchner and U.T. Mueller-Westerhoff, *J. Am. Chem. Soc.* **102**(2), 589 (1980).

34. J.D. Head and M.C. Zerner, *Chem. Phys. Lett.* **131**, 359 (1986).

35. W.P. Anderson, W.D. Edwards and M.C. Zerner, *Inorg. Chem.* **25**(16), 2728–2732 (1986).

36. W.D. Edwards and M.C. Zerner, *Theor. Chim. Acta* **72**, 347 (1987).

37. W.P. Anderson, T.R. Cundari, R.S. Drago and M.C. Zerner, *Inorg. Chem.* **29**(1), 1–3 (1990).

38. N. Mataga and K. Nishimoto, *Z. Phys. Chem. (Frankfurt)* **13**, 140 (1957).

# Figure Captions.

Figure 1. Reichardt's dye #1 (RB).

Figure 2. Reichardt's dye #1, conformer A, in gas phase. AM1 optimized geometry.

Figure 3. Reichardt's dye #1, conformer B, in gas phase. AM1 optimized geometry.

Figure 4. Reichardt's dye #1 (conformer B), in chloroform. AM1–SCRF-SM geometry.

Figure 5. Reichardt's dye #1 (conformer B), in methanol. AM1–SCRF-SM geometry.

Figure 6. Reichardt's dye #1 (conformer B), in water. AM1–SCRF-SM geometry.

Figure 7. Plot of theoretical vs. experimental results for the $E_T(30)$ parameter.

Table I Summary of AM1–SCRF results for Reichardt's dye #1 (RB).

| Medium | $\epsilon$ | Dihedral angles (°) | | | $\Delta H_f$ (kcal/mol) | $\mu$ (D) | IP (eV) |
|--------|-----------|-----------------|-----------------|-----------------|-------------|-----------|---------|
| | | $\xi$ 33-32-9-8 | $\phi$ 15-14-2-1 | $\chi$ 21-20-4-3 | | | |
| *Vaccuum* | | | | | | | |
| A | 1.000 | -39.0 | 128.4 | -37.9 | 202.8 | 13.005 | 6.938 |
| A' | 1.000 | -39.1 | -55.2 | -37.8 | 202.8 | 12.979 | 6.939 |
| B | 1.000 | -140.8 | -54.1 | -37.9 | 202.9 | 13.094 | 6.923 |
| *A Conformation* | | | | | | | |
| dioxane | 2.209 | -38.4 | 131.2 | -36.9 | 200.2 | 15.883 | 6.950 |
| ethanol | 24.30 | -38.1 | 130.0 | -34.4 | 195.4 | 19.064 | 7.046 |
| $CH_3OH$ | 32.63 | -38.1 | 130.0 | -34.4 | 195.3 | 19.121 | 7.052 |
| $CH_3CN$ | 35.94 | -38.0 | 130.0 | -34.4 | 195.2 | 19.134 | 7.054 |
| $H_2O$ | 78.54 | -38.1 | 129.9 | -34.4 | 195.0 | 19.225 | 7.062 |
| *A' Conformation* | | | | | | | |
| $CH_3OH$ | 32.63 | -38.1 | -52.9 | -34.5 | 195.3 | 19.116 | 7.053 |
| $CH_3CN$ | 35.94 | -38.1 | -52.9 | -34.5 | 195.2 | 19.129 | 7.054 |
| $H_2O$ | 78.54 | -38.1 | -54.3 | -34.4 | 195.1 | 19.191 | 7.062 |
| *B Conformation* | | | | | | | |
| dioxane | 2.209 | -140.8 | -53.9 | -37.9 | 200.0 | 14.905 | 6.963 |
| $CH_3OH$ | 32.63 | -141.7 | -52.7 | -34.6 | 195.1 | 19.131 | 7.043 |
| $CH_3CN$ | 35.94 | -141.7 | -52.7 | -34.6 | 195.1 | 19.146 | 7.044 |
| $H_2O$ | 78.54 | -141.7 | -52.9 | -34.4 | 194.8 | 19.267 | 7.052 |

Table II Calculated (gas phase) absorption spectrum of Reichardt's dye #1, conformer A.

| $\Delta E$ [a] $(cm^{-1})$ | $f_{osc.}$ [b] | Main CI contributions and single excitations |
|---|---|---|
| 11483 [c] | 0.405 | +0.96901 (102→103) (HOMO→LUMO) |
| 17138 [d] | 0.045 | -0.97468 (102→104) (HOMO→LUMO+1) |
| 24180 | 0.027 | -0.89879 (101→103) (HOMO-1→LUMO) |
| 25556 [e] | 0.478 | -0.69212 (102→107), -0.59668 (102→111) |
| 26418 | 0.054 | +0.61817 (102→105), +0.51282 (102→108) |
| 26951 | 0.022 | +0.75531 (102→110), +0.49626 (102→109) |
| 27550 | 0.016 | -0.74336 (102→108), -0.41459 (102→109) |
| 27784 | 0.038 | +0.63383 (102→111), -0.54800 (102→107) |
| 27900 | 0.058 | +0.83022 (100→103), -0.35859 (102→111) |
| 30085 [f] | 0.049 | +0.53846 (102→105), +0.52160 (99→103) |
| 31572 [f] | 0.305 | -0.73333 (96→103), +0.41061 (94→103) |
| 31719 [f] | 0.084 | -0.53730 (99→103), +0.46658 (102→105) |
| 31901 | 0.006 | +0.95613 (102→106) |
| 33515 [g] | 0.012 | +0.67122 (101→104), +0.48958 (102→113) |
| 33603 [g] | 0.047 | -0.58691 (102→113), +0.43957 (102→112) |
| 33871 [g] | 0.015 | +0.86539 (102→114) |
| 34264 [g] | 0.464 | +0.83022 (100→103), -0.35859 (102→111) |

a Transition energies. b Oscillator strengths: $f_{ij} = 4.7092 \times \Delta E_{ij} < i \mid \mu \mid j >^2$

c—g Experimental values in 1,4–dioxane [1]. (c) $12600 \ cm^{-1} = 795$ nm; (d) $21500 \ cm^{-1} = 465$ nm; (e) $25000 \ cm^{-1} = 400$ nm; (f) a shoulder at $31000 \ cm^{-1} = 322$ nm; (g) a broad band centered at approximately $33330 \ cm^{-1} = 300$ nm.

14

Table III Calculated (gas phase) absorption spectrum of Reichardt's dye #1, conformer B.

| $\Delta E$ [a] $(cm^{-1})$ | $f_{osc.}$ [b] | Main CI contributions and single excitations |
|---|---|---|
| 11218 [c] | 0.392 | +0.96687 (102→103) (HOMO→LUMO) |
| 16917 [d] | 0.045 | -0.97398 (102→104) (HOMO→LUMO+1) |
| 24688 | 0.016 | +0.85674 (101→103) (HOMO-1→LUMO) |
| 25187 [e] | 0.500 | +0.57067 (102→111), +0.59781 (102→107) |
| 26220 | 0.056 | -0.62569 (102→105), +0.52804 (102→108) |
| 26797 | 0.016 | +0.76846 (102→110), -0.45084 (102→109) |
| 27364 | 0.011 | -0.75341 (102→108), -0.44406 (102→109) |
| 27498 | 0.001 | -0.91681 (100→103) |
| 27558 | 0.052 | +0.74652 (102→111), -0.61248 (102→107) |
| 29895 [f] | 0.047 | +0.54909 (102→105), +0.50071 (99→103) |
| 31434 [f] | 0.291 | -0.79422 (96→103), -0.32512 (94→103) |
| 31567 [f] | 0.125 | +0.60065 (99→103), -0.43290 (102→105) |
| 31699 | 0.005 | +0.96039 (102→106) (HOMO→LUMO+3) |
| 33410 [g] | 0.052 | -0.87124 (102→112) |
| 33592 [g] | 0.002 | +0.77394 (102→114) |
| 33592 [g] | 0.002 | +0.87672 (101→104) (HOMO-1→LUMO+1) |
| 33887 [g] | 0.012 | -0.74600 (102→113), -0.41668 (102→114) |
| 34658 [g] | 0.529 | -0.31631 (95→107) |

a Transition energies. b Oscillator strengths: $f_{ij} = 4.7092 \times \Delta E_{ij} < i \mid \mu \mid j >^2$

c—g Experimental values in 1,4–dioxane [1]. (c) 12600 $cm^{-1}$ = 795 nm; (d) 21500 $cm^{-1}$ = 465 nm; (e) 25000 $cm^{-1}$ = 400 nm; (f) a shoulder at 31000 $cm^{-1}$ = 322 nm; (g) a broad band centered at approximately 33330 $cm^{-1}$ = 300 nm.

Table IV Calculated absorption spectrum of Reichardt's dye #1, conformer A in 1,4–dioxane.

| $\Delta E$ [a] $(cm^{-1})$ | $f_{osc.}$ [b] | Main CI contributions and single excitations |
|---|---|---|
| 10591 [c] | 0.153 | -0.97127 (102→103) (HOMO→LUMO) |
| 17640 [d] | 0.030 | -0.98076 (102→104) (HOMO→LUMO+1) |
| 25217 [e] | 0.414 | -0.75027 (102→111), -0.43925 (102→107) |
| 25611 [e] | 0.151 | +0.82156 (101→103), +0.37918 (100→103) |
| 27069 | 0.040 | +0.73119 (102→105), +0.48779 (102→110) |
| 27772 | 0.001 | -0.72349 (102→109), -0.59091 (102→107) |
| 27536 | 0.057 | -0.50022 (102→108), -0.49728 (102→109) |
| 27339 | 0.030 | +0.71390 (102→108), +0.34673 (102→111) |
| 28305 | 0.058 | -0.82669 (100→103), +0.45851 (101→103) |
| 31307 [f] | 0.342 | +0.75436 (96→103), -0.35847 (93→103) |
| 31842 [f] | 0.065 | +0.64745 (99→103), -0.35764 (95→103) |
| 31941 | 0.069 | +0.72591 (102→112), +0.47590 (102→113) |
| 32186 | 0.037 | +0.86755 (102→114) (HOMO→LUMO+11) |
| 32815 [g] | 0.429 | +0.65087 (102→113), -0.39108 (102→112) |
| 32655 [g] | 0.062 | -0.61304 (102→110), +0.47997 (102→105) |
| 33945 [g] | 0.057 | -0.74460 (101→104), -0.34662 (99→103) |
| 33290 [g] | 0.003 | -0.81896 (102→106), (HOMO→LUMO+3) |
| 34740 [g] | 0.319 | +0.56390 (95→103), -0.52880 (94→103) |

a Transition energies. b Oscillator strengths: $f_{ij} = 4.7092 \times \Delta E_{ij} <i \mid \mu \mid j>^2$

c—g Experimental values in 1,4–dioxane [1]. (c) 12,600 $cm^{-1}$ = 795 nm; (d) 21,500 $cm^{-1}$ = 465 nm; (e) a sharp peak at 25,000 $cm^{-1}$ = 400 nm; (f) a slight shoulder at 31,000 $cm^{-1}$ = 322 nm; (g) a broad band centered at approximately 33,330 $cm^{-1}$ = 300 nm.

Table V Calculated absorption spectrum of Reichardt's dye #1, conformer B in 1,4–dioxane.

| $\Delta E$ [a] $(cm^{-1})$ | $f_{osc.}$ [b] | Main CI contributions and single excitations |
| --- | --- | --- |
| 11871 [c] | 0.304 | -0.96922 (102→103) (HOMO→LUMO) |
| 18193 [d] | 0.041 | +0.97441 (102→104) (HOMO→LUMO+1) |
| 24925 [e] | 0.401 | +0.65478 (102→111), -0.63700 (102→106) |
| 26027 [e] | 0.162 | -0.91968 (101→103) |
| 27469 | 0.049 | -0.71689 (102→105), -0.53121 (102→110) |
| 27917 | 0.013 | +0.90477 (102→109) (HOMO→LUMO+6) |
| 27495 | 0.027 | -0.55251 (102→108), -0.53296 (102→111) |
| 27523 | 0.021 | +0.66714 (102→108), +0.45593 (102→111) |
| 27856 | 0.003 | -0.96844 (100→103) (HOMO-2→LUMO) |
| 31562 [f] | 0.145 | +0.68260 (99→103), -0.40201 (95→103) |
| 31938 [f] | 0.281 | -0.78945 (96→103) (HOMO-6→LUMO) |
| 32015 | 0.066 | -0.87926 (102→112) (HOMO→LUMO+9) |
| 32602 | 0.050 | +0.78754 (102→113) (HOMO→LUMO+10) |
| 33428 [g] | 0.195 | -0.57387 (102→114), +0.49714 (102→110) |
| 33474 [g] | 0.002 | +0.82964 (102→107) (HOMO→LUMO+4) |
| 34215 [g] | 0.238 | -0.67225 (102→107), -0.40388 (102→110) |
| 34863 [g] | 0.018 | +0.85915 (101→104) (HOMO-1→LUMO+1) |
| 35599 [g] | 0.201 | -0.46040 (94→103), -0.39471 (95→103) |

a Transition energies. b Oscillator strengths: $f_{ij} = 4.7092 \times \Delta E_{ij} < i \mid \mu \mid j >^2$

c—g Experimental values in 1,4–dioxane [1]. (c) 12,600 cm$^{-1}$ = 795 nm; (d) 21,500 cm$^{-1}$ = 465 nm; (e) a sharp peak at 25,000 cm$^{-1}$ = 400 nm; (f) a slight shoulder at 31,000 cm$^{-1}$ = 322 nm; (g) a broad band centered at approximately 33,330 cm$^{-1}$ = 300 nm.

Table VI First CT band in the UV-visible absorption spectrum of pyridinium-$N$-phenoxide betaines.

| Solvent | $\epsilon$ | $n_D$ | $\nu_{calcd.}$ (cm$^{-1}$) | | $\nu_{exptl.}$ (cm$^{-1}$) [3] | $E_T(30)$ (kcal) | |
|---|---|---|---|---|---|---|---|
| | | | SCRF | SCRF-SM | | Calcd. | Exptl. [3] |
| hexane | 1.890 | 1.3751 | 11,050 | ... | 10,850 | 31.6 | 31.0 |
| CCl$_4$ | 2.238 | 1.460 | 11,260 | ... | 11,338 | 32.2 | 32.4 |
| benzene | 2.284 | 1.501 | 11,297 | ... | 11,990 | 32.3 | 34.3 |
| 1,4-dioxane | 2.209 | 1.4224 | 11,231 | ... | 12,600 | 32.1 | 36.0 |
| CHCl$_3$ | 4.806 | 1.446 | 12,008 | 13,555 | 13,680 | 38.8 | 39.1 |
| CH$_3$CN | 35.94 | 1.3442 | 12,831 | ... | 16,077 | ... | 45.6 |
| methanol | 32.63 | 1.3288 | 12,246 | 19,272 | 19,420 | 55.1 | 55.4 |
| water | 78.54 | 1.3328 | 12,370 | 21,790 | 22,075 | 62.3 | 63.0 |

## Table VII Calculated absorption spectrum of Reichardt's dye #1, conformer B in chloroform, SM approximation.

| $\Delta E$ [a] (cm$^{-1}$) | $f_{osc.}$ [b] | Main CI contributions and single excitations |
|---|---|---|
| 13555 [c] | 0.013 | -0.95917 (154→155) (HOMO→LUMO) |
| 16260 | 0.074 | +0.98861 (154→158) (HOMO→LUMO+3) |
| 16451 | 0.101 | +0.98535 (154→159) (HOMO→LUMO+4) |
| 17943 | 0.009 | +0.98031 (154→156) (HOMO→LUMO+1) |
| 19979 | 0.002 | -0.96406 (154→157) (HOMO→LUMO+2) |
| 22236 | 0.019 | +0.97694 (154→160) (HOMO→LUMO+5) |
| 26355 | 0.484 | -0.79421 (154→165) (HOMO→LUMO+10) |
| 26465 | 0.013 | -0.71339 (153→155) (HOMO-1→LUMO) |

a Transition energies. b Oscillator strengths: $f_{ij} = 4.7092 \times \Delta E_{ij} <i \mid \mu \mid j>^2$

c Exptl. value 13,680 cm$^{-1}$ = 833 nm

Table VIII Calculated absorption spectrum of RB, conformer A in methanol, SM approximation.

| $\Delta E$ [a] $(cm^{-1})$ | $f_{osc.}$ [b] | Main CI contributions and single excitations |
|---|---|---|
| 15071 | 0.038 | +0.96651 (130→131) (HOMO→LUMO) |
| 19224 [c] | 0.103 | +0.88285 (129→131) (HOMO-1→LUMO) |
| 20815 | 0.077 | -0.89996 (130→132) (HOMO→LUMO+1) |
| 23335 | 0.037 | +0.83438 (129→132) (HOMO-1→LUMO+1) |
| 24431 | 0.442 | -0.76913 (130→136) (HOMO→LUMO+5) |
| 27449 | 0.032 | -0.92785 (130→134) (HOMO→LUMO+3) |

a Transition energies. b Oscillator strengths. c Exptl. 19,420 $cm^{-1}$ = 515 nm.

Table IX Calculated absorption spectrum of RB, conformer B in methanol, SM approximation.

| $\Delta E$ [a] $(cm^{-1})$ | $f_{osc.}$ [b] | Main CI contributions and single excitations |
|---|---|---|
| 14138 | 0.020 | -0.96546 (130→131) (HOMO→LUMO) |
| 19320 [c] | 0.164 | +0.94352 (129→131) (HOMO-1→LUMO) |
| 21343 | 0.044 | -0.96346 (130→132) (HOMO→LUMO+1) |
| 24052 | 0.442 | -0.76055 (130→136) (HOMO→LUMO+5) |
| 24929 | 0.031 | +0.81435 (129→132) (HOMO-1→LUMO+1) |
| 28427 | 0.040 | +0.69131 (130→133) (HOMO→LUMO+2) |

a Transition energies. b Oscillator strengths. c Exptl. 19,420 $cm^{-1}$ = 515 nm.

Table X Calculated absorption spectrum of RB, conformer A in water, SM approximation.

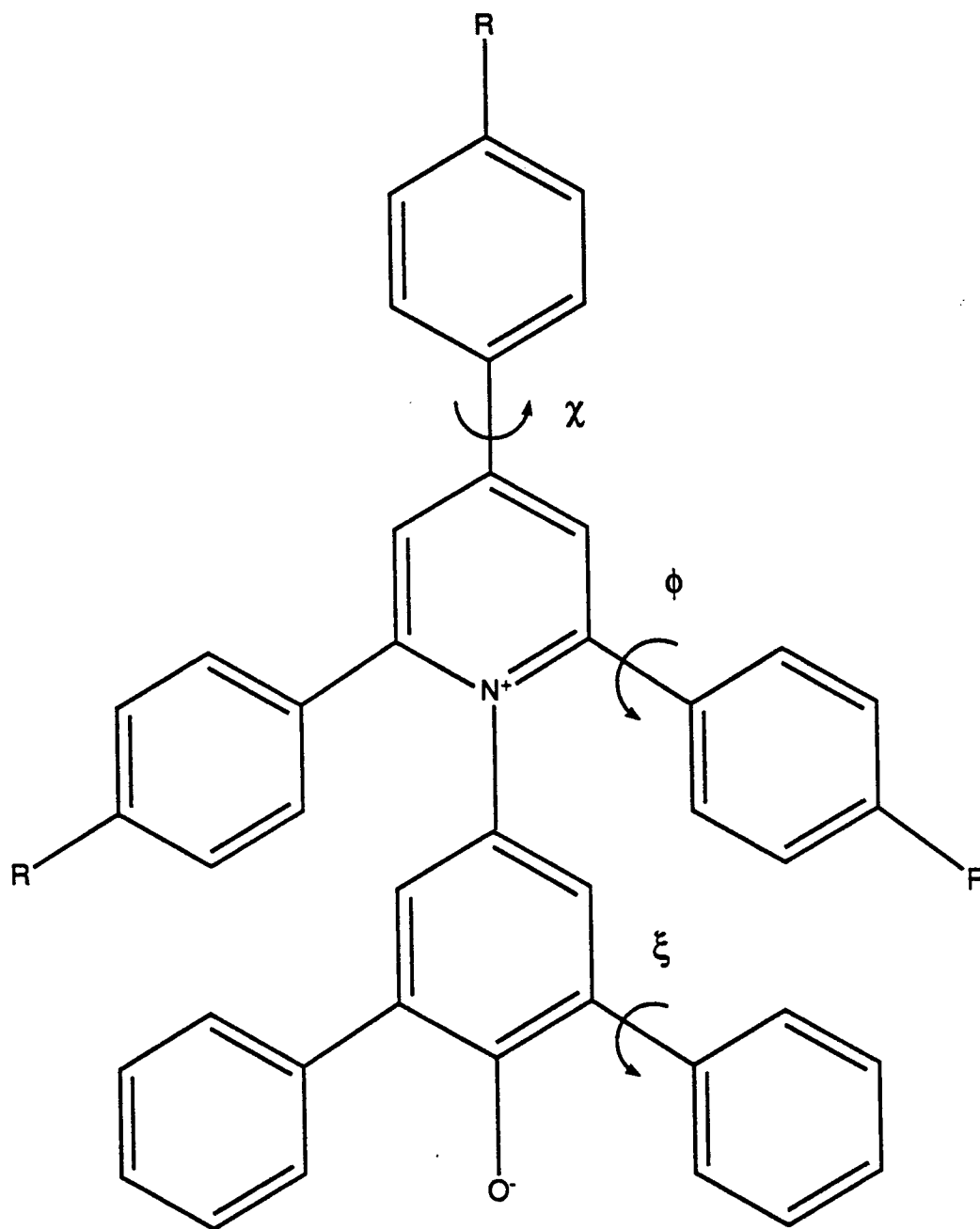| $\Delta E$ [a] $(cm^{-1})$ | $f_{osc.}$ [b] | Main CI contributions and single excitations |
|---|---|---|
| 14061 | 0.017 | +0.97387 (118→119) (HOMO→LUMO) |
| 21851 [c] | 0.035 | -0.97906 (118→120) (HOMO→LUMO+1) |
| 23000 | 0.168 | +0.89137 (115→119) (HOMO-3→LUMO) |
| 24377 | 0.470 | -0.83016 (118→124) (HOMO→LUMO+5) |
| 26658 | 0.003 | +0.76182 (115→120) (HOMO-3→LUMO+1) |
| 28836 | 0.070 | +0.74919 (118→122) (HOMO→LUMO+3) |
| 29450 | 0.016 | -0.66650 (118→121) (HOMO→LUMO+2) |

a Transition energies. b Oscillator strengths. c Exptl. 22,075 $cm^{-1}$ = 543 nm.

Table XI Calculated absorption spectrum of RB, conformer B in water, SM approximation.

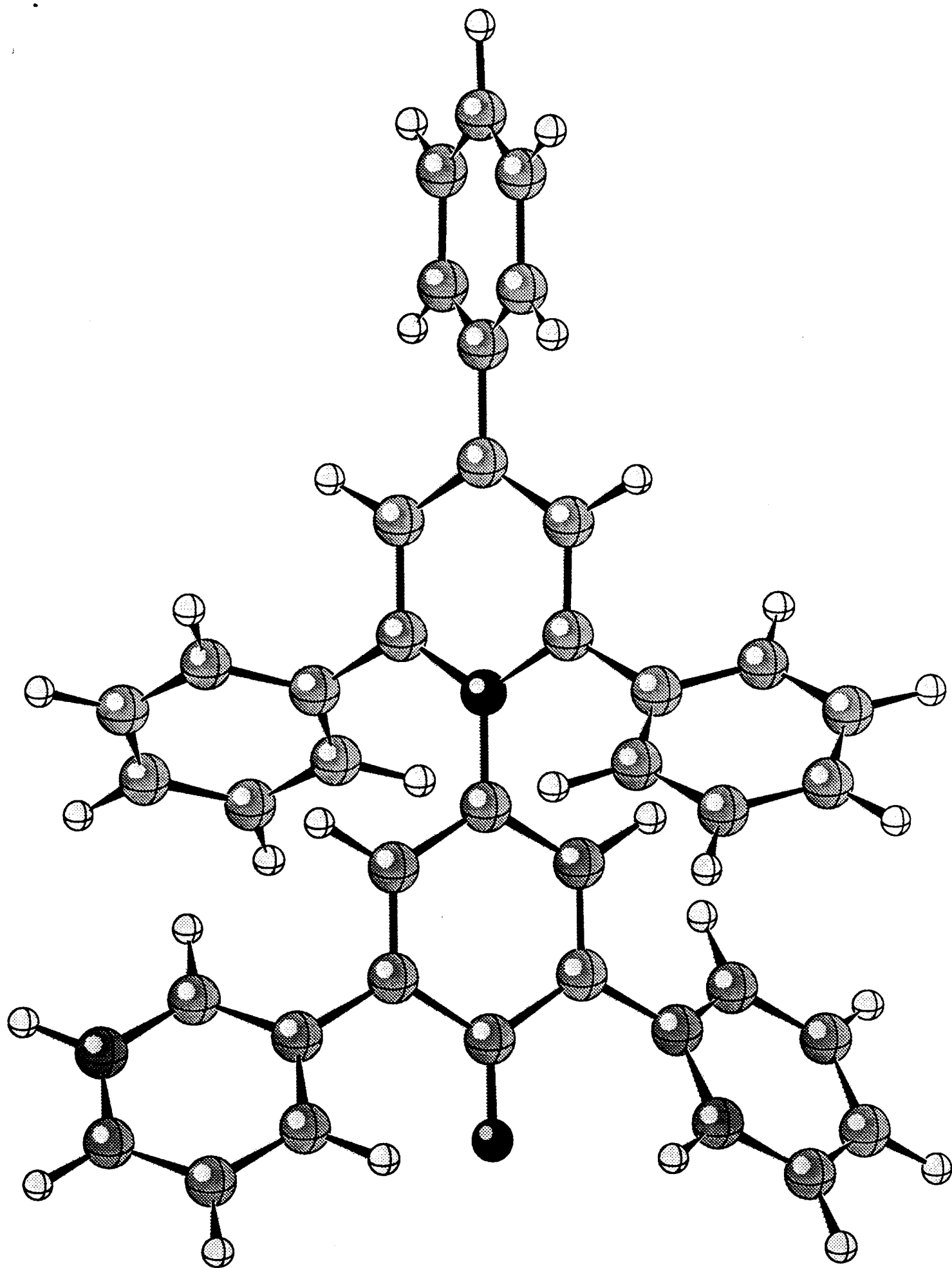| $\Delta E$ [a] $(cm^{-1})$ | $f_{osc.}$ [b] | Main CI contributions and single excitations |
|---|---|---|
| 13978 | 0.018 | +0.97253 (118→119) (HOMO→LUMO) |
| 21728 [c] | 0.037 | -0.97587 (118→120) (HOMO→LUMO+1) |
| 23029 | 0.172 | +0.91992 (115→119) (HOMO-3→LUMO) |
| 24056 | 0.450 | +0.87774 (118→124) (HOMO→LUMO+5) |
| 26674 | 0.003 | +0.78160 (115→120) (HOMO-3→LUMO+1) |
| 28325 | 0.072 | +0.87366 (118→122) (HOMO→LUMO+3) |
| 29288 | 0.009 | -0.83416 (118→121) (HOMO→LUMO+2) |

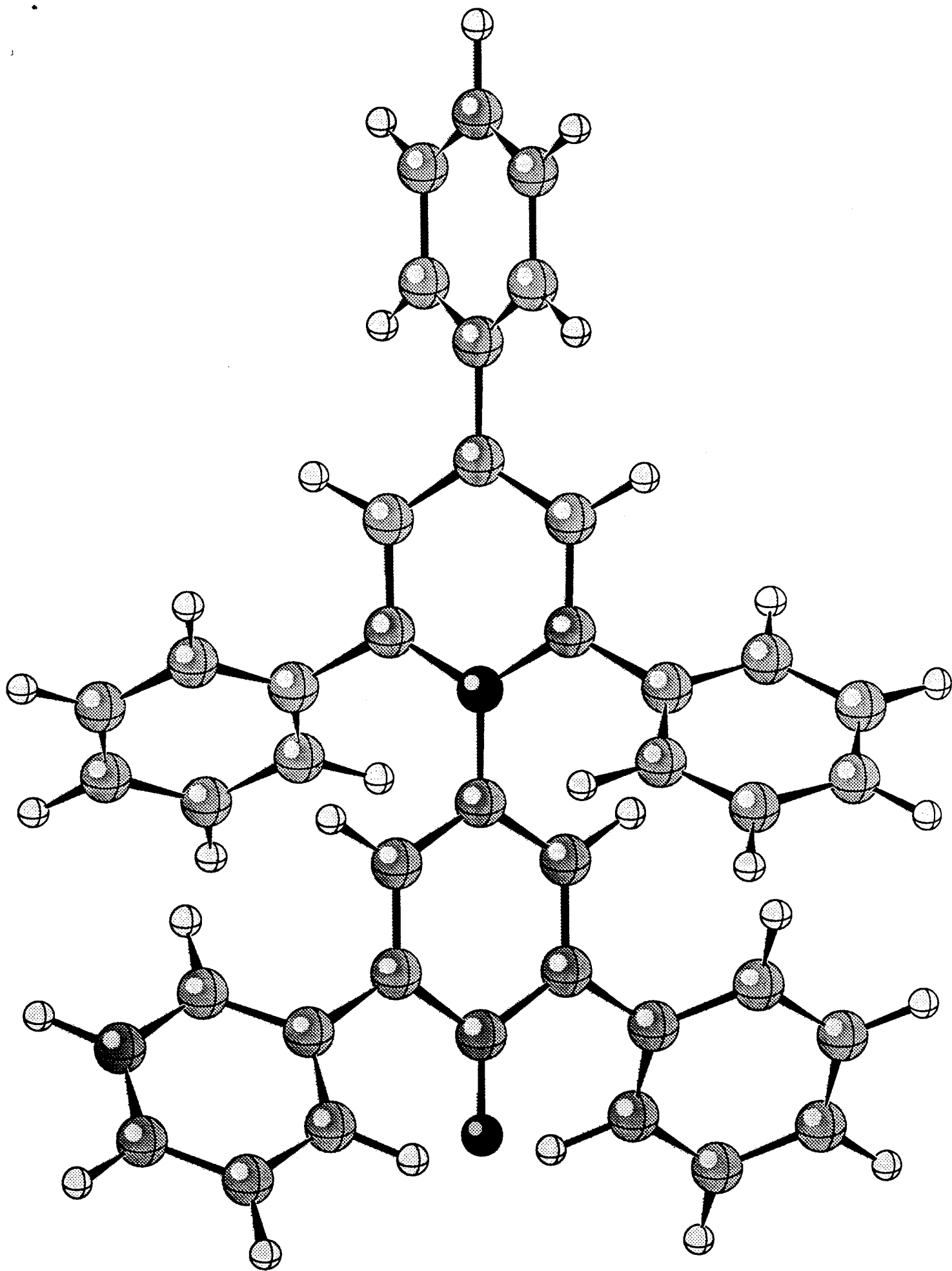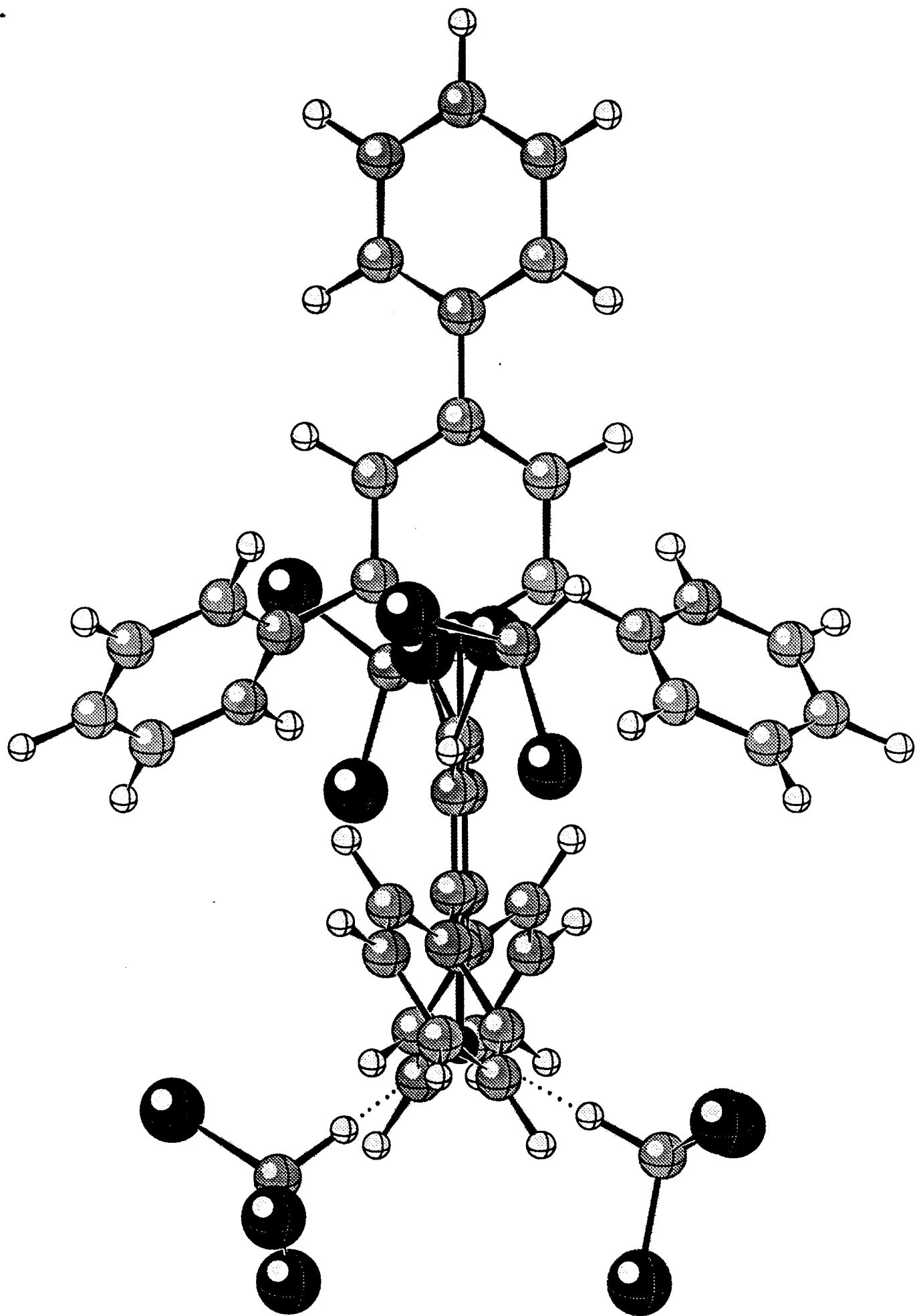a Transition energies. b Oscillator strengths. c Exptl. 22,075 $cm^{-1}$ = 543 nm.

Fig. 1



dye #1, R = H

dye #2, R = SO₂CH₃

Fig. 4

Et(30) as calculated by INDO/S

Calcd. (kcal/mol)

Exptl. (kcal/mol)

H2O

CH3OH

CHCl3

1,4-dioxane

CCl4